IMECE2018-86582

LOW-TEMPERATURE ENERGY EFFICIENCY OF LITHIUM-ION BATTERIES

Ashkan Nazari
Center For Tire Research (CenTiRe)
Mechanical Engineering
Department, Virginia Tech
Blacksburg, VA, United States

Roja Esmaeeli
Advanced Energy & Sensor Lab.,
Mechanical Engineering
Department, University of Akron
Akron, OH, United States

Seyed Reza Hashemi
Advanced Energy & Sensor
Lab., Mechanical Engineering
Department, University of Akron
Akron, OH, United States

Haniph Aliniagerdroudbari
Advanced Energy & Sensor
Lab., Mechanical Engineering
Department, University of Akron
Akron, OH, United States

Siamak Farhad[1]
Advanced Energy & Sensor Lab.,
Mechanical Engineering
Department, University of Akron
Akron, OH, United States

ABSTRACT

In this study, the low-temperature energy efficiency of lithium-ion batteries (LIBs) with different chemistries and nominal capacities at various charge and discharge rates is studied through multi-physics modeling and computer simulation. The model is based on the irreversible heat generation in the battery, leading to the charge/discharge efficiency in LIBs with graphite/LiFePO$_4$, graphite/LiMn$_2$O$_4$, and graphite/LiCoO$_2$ electrode materials in which the effects of the battery nominal capacity at various charge and discharge rates are studied. Using characterized sources of the heat generation in the LIB leads to providing a battery efficiency plot at different operation condition for each LIBs. The results of this study assist the battery engineers to have much more accurate prediction over the efficiency of the LIBs at low temperatures.

INTRODUCTION

Lithium-ion batteries (LIBs) possess several features that made them the most popular type of rechargeable electrical energy storage system in market [1]. High operating voltage, high energy & power, good cycling performance, low self-discharge and no memory effect made these batteries suitable for many applications including portable electronic [2]. Generally, a LIB is shaped of two electrodes (anode and cathode) that are usually mechanically supported by metallic current collectors as well as the electrolyte that allows lithium-ion transfer between electrodes which the behavior is characterized based on the theory of the operation of porous electrodes developed by Newman [3]. In LIBs, Li-ions transport from one electrode to the other, while at the same time allowing electrons flow through an external circuit connected to the battery [4]. The anode and cathode are electrically insulated from one another by a polymer separator, which is permeable to Li-ions but not to electrons. Since LIBs are being used in wide range of operation temperature, with regard to the cold season in North America, they should be designated optimally to maintain the desired performance at low temperatures. From the basic characteristics of large-scale LIBs, particularly those used as energy storage devices in grid systems and EVs, such as voltage, current, and capacity, more comprehensive analysis requires concerning the macroscopic properties of LIB such as energy efficiency at low temperatures. Accordingly, energy efficiency plays key role in evaluating the working conditions of LIBs and represents the utilization of chemical energy stored in LIB at discharge or the utilization of electrical energy toward storing chemical energy in LIB at charge [5]. Also, the considerable importance of LIB's performance, leads a large number of researcher to conduct study in this field and provide new approach to assist this topic [6-13]. The goal of this study is to calculate the LIB energy efficiency at charge/discharge, using electrochemistry and electrical theory. Since the amount of electrochemical energy (EE) at discharge and the amount of electrical energy (E) dissipated at charge, change to heat, the irreversible heat generation is calculated to predict the LIB energy efficiency at charge/discharge. Studies on

---

[1] Corresponding Author (sfarhad@uakron.edu)

low-temperature behaviors of LIBs have been more focused on experimental measurements and observations while in the recent years multiphysics modeling and computer simulation have provided more understanding over cell behavior at low temperature. Li et al. conducted an experimental investigation on lithium titanate battery (LTO) energy efficiency which is utilized as the energy storage device in micro-grid. They have provided a quantitative relationship of OCV and SOC using non-linear curve fitting to calculate energy efficiency of a single cell [14]. Schimpe et al. provided an electro-thermal model for stationary lithium-ion battery container storage system to analyze the system energy efficiency [15]. Meister et al. investigated the efficiency of LIBs with different active materials and provided a comprehensive comparison over anode and cathode materials with respect to their electrochemical characteristics [16]. Toman et al. presented a methodology to measure the LIB's efficiency with regard to charge/discharge current, leading to an analytical overall energy storage efficiency against current [17].

In this study, the LIB's energy efficiency at low temperature of -20˚C is investigated through multi-physics modeling and computer simulation, contributing the thermal management system of the LIB to keep the battery's temperature at desired range to obtain the maximum energy efficiency at charge/discharge [18-21].

NOMENCLATURE

Symbols	Discretion
a	specific interfacial area, $m^2 m^{-3}$
c	charge
$c1$	concentration of lithium ion in solid, $mol m^{-3}$
$c2$	concentration of the binary electrolyte, $mol m^{-3}$
d	discharge
E	electrical energy Jm^{-3}
F	Faraday's constant, 96,487 $sAmol^{-1}$
i	battery current, Am^{-2}
irr	irreversible
J	local pore wall flux of lithium ions, $mol\ m^{-2}\ s^{-1}$
k	electrochemical reaction rate constant, $m^{2.5}\ mol^{-0.5}$ ${}_{\text{s}}$
Q	heat generation Jm^{-3}
R	gas constant, 8.3145 $Jmol^{-1}\ K^{-1}$
T	temperature, K
T_{ref}	reference temperature
t	time, s
$t+$	transference number of lithium ion
U	open-circuit potential, V
$U{i,ref}$	open circuit potential of electrode i under the refere
V	battery voltage ,V
x	spatial coordinate

Greek Letters

σ_i	electronic conductivity of solid matrix, Sm^{-1}
φ_1	potential in the solid phase, V
φ_2	potential in the electrolyte, V
δ	thickness, m
η	Efficiency

Subscripts

1	solid phase
2	liquid phase
cc	current collector
in	input
ohm	ohmic
out	output

Acronyms

CC	Current collector
E	Electrical Energy
EE	Electrochemical Energy
LFP	Lithium Iron Phosphate
LMO	Lithium Manganese Oxide
LCO	Lithium Cobalt Oxide
Sep	Separator

MODELING
Porous electrode model

In order to simulate the performance of the LIBs, first the battery charge and discharge process is conducted through multiphysics modeling. The list of the equations used for the modeling as well as the standard potential and temperature derivative of standard potential of the electrodes are provided in [22]. Based on the Newman's [3] pseudo-two-dimensional (P2D) model, porous-electrode and concentrated solution model is developed. In addition, White's heat generation model [23] is used to characterize the heat sources in LIB. The model is assumed isothermal as the temperature difference between the hottest and coldest spots of an operating LIB is negligible or if it is significant it is controlled via a battery thermal management system (TMS) to minimize this temperature difference [24].

Eqs. 1-3 show the lithium ions deintercalating from the cathode during charging and inserted into the anode. Reversely, during discharge, lithium ions are extracted from the anode and intercalated into the cathode.

$$Li_x FePO_4 \rightleftharpoons Li_{x-\delta} FePO_4 + \delta Li^+ + \delta e^- \text{ (cathode)} \quad (1)$$
$$Li_y C_m + \delta Li^+ + \delta e^- \rightleftharpoons Li_{y+\delta} C_m \text{ (anode)}$$

$$Li_x Mn_2 O_4 \rightleftharpoons Li_{x-\delta} Mn_2 O_4 + \delta Li^+ + \delta e^- \text{ (cathode)} \quad (2)$$
$$Li_y C_6 + \delta Li^+ + \delta e^- \rightleftharpoons Li_{y+\delta} C_6 \text{ (anode)}$$

$$Li_x CoO_2 \rightleftharpoons Li_{x-\delta} CoO_2 + \delta Li^+ + \delta e^- \text{ (cathode)} \quad (3)$$
$$Li_y C_6 + \delta Li^+ + \delta e^- \rightleftharpoons Li_{y+\delta} C_6 \text{ (anode)}$$
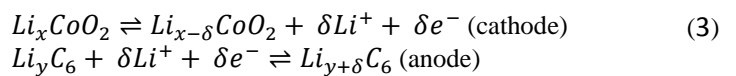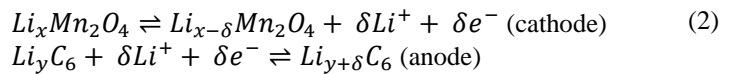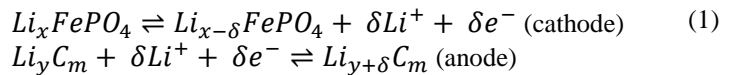
Charge and discharge of LIBs is associated with energy dissipation which is indicated in shape of heat generation. In fact,

the heat generated during charge/discharge in each part of the LIBs namely anode, cathode, separator and current collector are the summation of heat sources in those parts. List of the equations to calculate the heat in each part is provided in Table 1. In the porous electrode, the heat generation sources are categorized to three parts. The first part is the ohmic heat which originates from the electronic resistance and ionic resistance in the porous electrode. 2nd and 3rd heat sources in the porous electrode are the active polarization and concentration polarization heat caused by concentration gradients that are built up in the electrolyte and in the solid phase.

Table 1. Multiphysics model equations used to simulate heat generation in LIBs [5]

Heat Equations in LIBs	Description
$Q_{cc} = \sigma_{cc} \left(\frac{\partial \phi_1}{\partial x} \right)^2$	Ohmic heat in CC
$Q_{sep} = \kappa_{eff,i} \left(\frac{\partial \phi_2}{\partial x} \right)^2 + \frac{2RT(1 - t_+^0)}{F} \frac{\partial}{\partial x} \left(\kappa_{eff,i} \frac{\partial(\ln c_i)}{\partial x} \right) \frac{\partial \phi_2}{\partial x}$	Ohmic heat in Sep
$Q_{ohm} = \sigma_{eff} \left(\frac{\partial \phi_1}{\partial x} \right)^2 + \kappa_{eff} \left(\frac{\partial \phi_2}{\partial x} \right)^2 + \frac{2RT(1 - t_+^0)}{F} \frac{\partial}{\partial x} \left(\kappa_{eff,i} \frac{\partial(\ln c_i)}{\partial x} \right) \frac{\partial \phi_2}{\partial x}$	Ohmic heat in electrode
$Q_{rxn} = FaJ(\phi_{1,i} - \phi_{2,i} - U_i)$	Polarization heat in electrode

To model the heat generation in G/LFP, G/LMO and G/LCO LIBs it is required to know the standard potentials and the temperature derivative of standard potentials of the graphite anode and LFP, LMO and LCO cathodes at different states of charge (SOC). The temperature dependent open-circuit potential of electrodes is approximated by Taylor's first order expansion around a reference temperature shown in Eq. 4. $U_{i,ref}$ is the open circuit potential at the reference temperature T_{ref} which the corresponding data is obtained from literature [22].

$$U_i = U_{i,ref} + (T - T_{ref}) \left[\frac{dU}{dT} \right] \quad (4)$$

LIB Efficiency at Charge and Discharge

There exist several ways to calculate the battery charge and discharge efficiencies, however, since the LIB efficiency in drive cycle is the main application of this study, the reversibility in charge and discharge process cancel each other. Accordingly, to calculate the LIB efficiency, the input and output electrical energy and the total irreversible heat generation during charge and discharge should be considered. The input electrical energy to the battery (J/m^3) during the charging process from time 0 to t is calculated from the following equation [5]:

$$E_{in/out} = \frac{1}{\delta} \int_0^t V_{c/d} \, i_{c/d} \, dt \quad (5)$$

where, δ is the summation of cell components' thickness including negative current collector, positive current collector, anode, cathode and separator. The heat generation during charge/discharge time t is also obtained from Eq. 6 and Eq. 7 [5].

$$Q_{heat,irr,c} = \int_0^t \frac{1}{\delta} \left(\int_0^\delta \dot{Q}'''_{heat,irr,c} \, dx \right) dt \quad (6)$$

$$Q_{heat,irr,d} = \int_0^t \frac{1}{\delta} \left(\int_0^\delta \dot{Q}'''_{heat,irr,d} \, dx \right) dt \quad (7)$$

where, $\dot{Q}'''_{heat,irr,c/d}$ is the local rate of total irreversible heat generation per unit volume during charge/discharge process. Based on the heat generation from Eq. 6 and Eq. 7 the charge and discharge efficiencies are defined in Eq. 8 and Eq. 9. In fact the energy that is stored in the battery is equal to the input electrical energy that is going to get into the battery minus the heat generated during the charge process. In addition, the stored energy is equal to electrical energy that comes out of the battery plus the heat dissipated to environment during discharge process.

$$\eta_c = 1 - \frac{Q_{heat,irr,c}}{E_{in}} \quad (8)$$

$$\eta_d = \frac{E_{out}}{E_{out} + Q_{heat,irr,d}} \quad (9)$$

The multiphysics model developed for this study was validated. The detail explanation of the validation has been explained in the other author's paper [5]. The model was run at constant current discharges at C-rate 1C at different temperatures. The comparison between the model and experimental cell voltage results are shown in [5] which the modeling results have a very good agreement with the experimental results with the maximum error of less than 3%.

The model parameters are listed in Table 2.

Table 2. Input parameters used for the multiphysics model.

Parameter	G/LFP	G/LMO	G/LCO
Cell temperature, K	253.15 [b]	253.15 [b]	253.15 [b]
Reference temperature	298.15	298.15	298.15
Theoretical capacity of anode, mol/m³	31507 [d]	31500 [d]	31858 [d]
Theoretical capacity of cathode, mol/m³	22806 [d]	22896 [d]	49943 [d]
Initial state-of-charge, cathode, mol/m³	20999 [c]	5808 [b]	48571 [d]
Initial state-of-charge, anode, mol/m³	1601 [c]	22045 [b]	1682 [d]
Thickness of separator, µm	25 [a]	76 [25]	25 [26]
Thickness of anode current collector, µm	8.5 [a]	12 [25]	8.5 [26]
Thickness of cathode current collector, µm	10 [a]	12 [25]	10 [26]
Initial electrolyte salt concentration, mol/m³	1000 [b]	1200 [25]	1000 [26]
High cut off Voltage, V	3.6 [c]	4.2 [b]	4.2 [b]
Low cut off Voltage, V	2.4 [c]	2.8 [b]	3.3 [b]

Particle radius, anode, m	3.5e-6 [a]	12.5e-6 [25]	6.5e-6 [26]
Particle radius, cathode, m	0.6e-6 [a]	8.5e-6 [25]	5.25e-6 [26]
Solid phase volume fraction, cathode	0.486 [a]	0.43 [25]	0.55 [26]
Bruggeman coefficient for tortuosity, cathode	1.5 [c]	1.5 [25]	1.5 [26]
Bruggeman coefficient for tortuosity, anode	1.5 [c]	1.5 [25]	1.5 [26]
Bruggeman coefficient for tortuosity, separator	1.5 [c]	1.5 [25]	1.5 [26]
Solid phase volume fraction, anode	0.4 [a]	0.384 [25]	0.505 [26]
Electrolyte phase volume fraction in cathode	0.365 [a]	0.4 [25]	0.3 [26]
Electrolyte phase volume fraction in anode	0.6 [a]	0.44 [25]	0.4382 [26]
Electrolyte phase volume fraction in separator	0.55 [a]	0.59 [25]	0.45 [26]
Reaction rate coefficient in cathode, m/s	5e-10 [c]	5e-10 [c]	6.66e-11 [26]
Reaction rate coefficient in anode, m/s	8.19e-12 [c]	2e-11 [c]	1.764e-11 [26]
Electrical conductivity in cathode, S/m	91	3.8	10 [26]
Electrical conductivity in anode, S/m	100	100	100 [26]
Electrical conductivity in Al, S/m	3.774e7	3.774e7	3.774e7
Electrical conductivity in Cu, S/m	5.998e7	5.998e7	5.998e7
Transfer coefficient in cathode	0.5 [c]	0.5 [c]	0.5 [c]
Transfer coefficient in anode	0.5 [c]	0.5 [c]	0.5 [c]
Contact resistant BTW electrode & CC, $\Omega.m^2$	0 [2 c]	0.025 [2 c]	0.03 [2 c]
Diffusion coefficient in cathode, m^2/s	3.2e-13 [c]	1e-14×exp(-1.434) [25, 27]	1e-11 [26]

[a] Measured

[b] Assumed

[c] Obtained by fitting to experimental data

[d] Based on theory

RESULTS AND DISCUSSION

In this part, the simulation results for the LIB efficiency with different chemistry of graphite/LiFePO$_4$ (G/LFP), graphite/LiMn$_2$O$_4$ (G/LMO) and graphite/LiCoO$_2$ (G/LCO) electrode materials at a very low temperature of -20˚C and different nominal capacities (2, 8, 12, 24 and 30 Ah/m^2) are presented. The cell temperature remains constant and uniform during charge and discharge. As it is explained in the modeling section, the battery efficiency is derived, using the irreversible heat generation in LIB. The irreversible heat is shaped from three polarizations heat sources namely, activation, concentration, and ohmic polarizations.
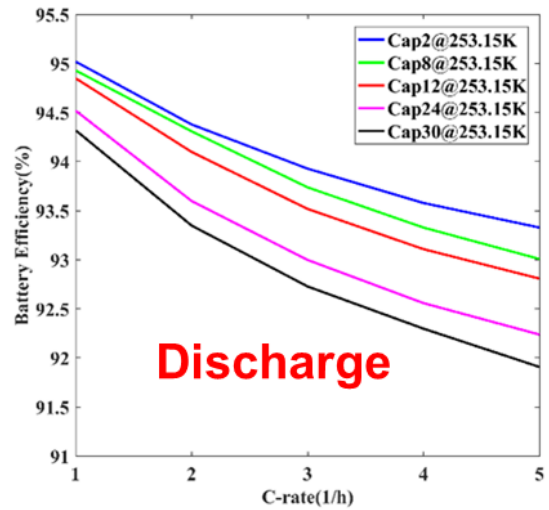

Figure 1. G/LFP LIB efficiency at different nominal capacities (Ah/m^2) and discharge rate at -20 ˚C

As it is shown in Fig. 1-6 the LIBs efficiencies are considerably effected by the rate of charge and discharge. In addition, the LIB's capacity plays a crucial role in charge and discharge efficiency. As shown in Fig 1-6 the LIB's efficiency decrease with charge/discharge rate.
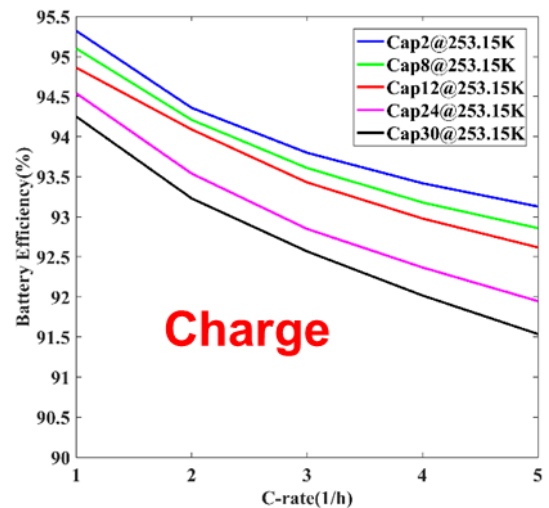

Figure 2. G/LFP LIB efficiency at different nominal capacities (Ah/m^2) and charge rate at -20 ˚C

In addition, the LIB's efficiency at charge/discharge decreases as the capacity increases. However, the rate of irreversible heat generation in LIBs with different electrodes and operation condition is different. Accordingly, different efficiency from each LIB at different operation condition is expected.
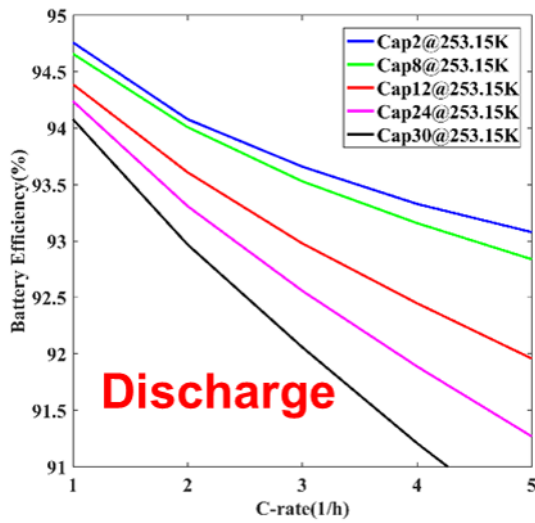
Figure 3. G/LMO LIB efficiency at different nominal capacities (Ah/m²) and discharge rate at -20 ˚C

As it is depicted in Fig. 2 and Fig. 3, the LIBs with G/LFP electrodes generally show nearly the same behavior at charge and discharge due to the fact that the rates of irreversible heat generation at charge and discharge are nearly the same. G/LMO LIB shows different behavior at charge at discharge. As it shown in Fig. 4 and Fig. 5, G/LMO LIBs possess more efficiency at discharge than charge due the fact the irreversible heat generated at charge is more than that of discharge. The details of the origin of the irreversible heat at charge/discharge is elaborated in [22]
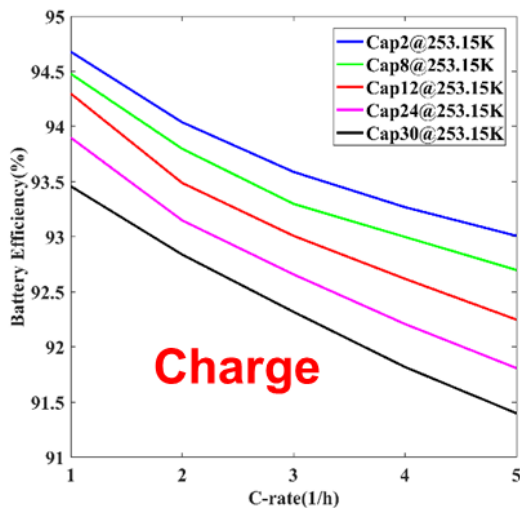

Figure 4. G/LMO LIB efficiency at different nominal capacities (Ah/m²) and charge rate at -20 ˚C

In LIBs with G/LCO electrodes the at low charge/discharge rate the LIB show nearly the same behavior, however at high charge/discharge G/LCO LIBs shows different behavior toward possessing more efficiency at discharge than charge. From the result obtained in this work and those of presented in [5] it is

obvious that generally the LIBs at very low temperature lose portion of the performance for the fact that the rate of mass transport decreased while the activation loss during charge/discharge increase which translates to the increased rates of the irreversible heat generation at charge/discharge.
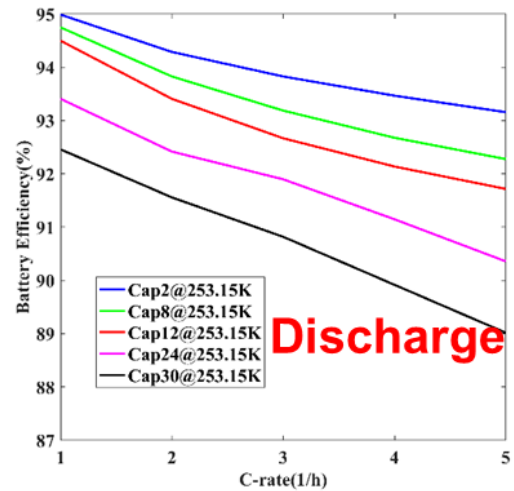

Figure 5. G/LCO LIB efficiency at different nominal capacities (Ah/m²) and discharge rate at -20 ˚C

Since the electrolyte in all three LIBs with different cathodes are the same, it is obvious that the particle size in the cathode plays a crucial role for LIBs to remain close to the charge/discharge efficiency of room temperature. Furthermore, for operation at −20˚C, decreasing the graphite particle radius is very effective to enhance cell performance. Diffusion coefficient in G/LCO LIBs is a key factor to remain the LIBs efficiency at very low temperature, as well. As it shown in this work, although the reaction rate coefficient in LCO battery's cathode is less than that of LMO and LFP, diffusion coefficient in cathode of LCO battery compensates this loss considerably.
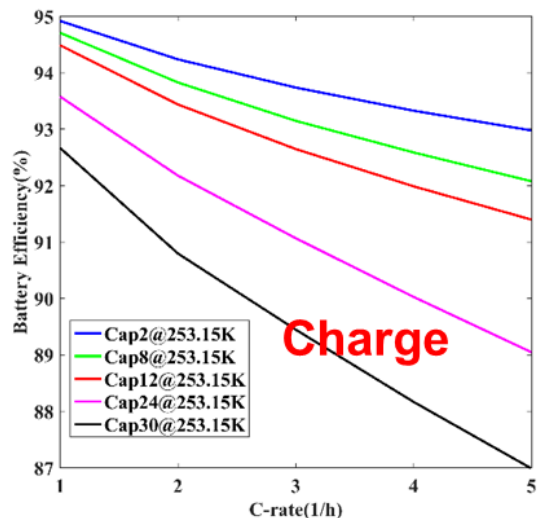

Figure 6. G/LCO LIB efficiency at different nominal capacities (Ah/m²) and charge rate at -20 ˚C

Copyright © 2018 by ASME

CONCLUSIONS

A validated mathematical model was employed to simulate the charge/discharge low-temperature energy efficiency of G/LFP, G/LMO and G/LCO LIBs with various nominal capacities. Several studies including the contribution of irreversible heat generation in battery to shape the LIB energy efficiency at different nominal capacities, C-rates at -20 ˚C are conducted. The low-temperature charge/discharge energy efficiency of G/LFP, G/LMO and G/LCO LIBs decreases with an increase in rate of charge/discharge. The energy efficiency also decreases with an increase in cell nominal capacity. Overall, in the range of investigation, the LIB chemistry, nominal capacity and C-rate may affect the low-temperature charge or discharge energy efficiency of LIBs up to 9-point%. For batteries with high nominal capacities charged/discharged at low C-rates (energy cells), the efficiency of G/LFP is the highest, followed by G/LMO and G/LCO. The same trend is observed for batteries with low nominal capacities charged/discharged at high C-rates (power cells). Since the energy efficiency depends on not only chemistry, but also the microstructure of electrodes such as thickness, particle size, volume fraction as well as composition of electrolyte, generally, G/LFP LIB provides better performance according to its microstructure parameters. The energy efficiency of G/LCO LIB is more sensitive to the change of C-rate in compression to G/LFP and G/LMO LIBs. For instance, the energy efficiency of a G/LFP with the nominal capacity of 30 Ah/m^2 discharged at C-rate of 5 is 3.5-point% less than the one discharge at C-rate of 1. In the future work, the sensitivity of the LIB's performance to the microstructure parameters at low temperatures will be investigated.

ACKNOWLEDGEMENT

REFERENCES

[1] Lu, Jun, Wu, Tianpin, and Amine, Khalil. "State-of-the-art characterization techniques for advanced lithium-ion batteries." *Nature Energy* Vol. 2 No. 3 (2017): pp. 17011.

[2] Scrosati, Bruno, and Garche, Jürgen. "Lithium batteries: Status, prospects and future." *Journal of Power Sources* Vol. 195 No. 9 (2010): pp. 2419-2430.

[3] Newman, John, and Tiedemann, William. "Porous-electrode theory with battery applications." *AIChE Journal* Vol. 21 No. 1 (1975): pp. 25-41.

[4] Kazemiabnavi, Saeed, Malik, Rahul, Orvananos, Bernardo, Abdellahi, Aziz, Ceder, Gerbrand, and Thornton, Katsuyo. "The Effect of Surface-Bulk Potential Difference on the Kinetics of Intercalation in Core-Shell Active Cathode Particles." *Journal of Power Sources* Vol. 382 (2018): pp. 30-37.

[5] Nazari, Ashkan, Esmaeeli, Roja , Hashemi, Seyed Reza, Aliniagerdroudbari, Haniph, and Farhad, Siamak. "The Effect of Temperature on Lithium-Ion Battery Energy Efficiency with Graphite/LiFePO4 Electrodes at Different Nominal Capacities." *Proceedings of the ASME 2018 Power and Energy Conference* Lake Buena Vista, FL, USA, June 24-28, 2018.

[6] Nazari, Ashkan, Derakhshi, Amin Zadkazemi, Nazari, Arash, and Firoozabadi, Bahar. "Drop formation from a capillary tube: Comparison of different bulk fluid on Newtonian drops and formation of Newtonian and non-Newtonian drops in air using image processing." *International Journal of Heat and Mass Transfer* Vol. 124 (2018): pp. 912-919.

[7] Hashemi, Seyed Reza, Nazari, Ashkan, Esmaeeli, Roja, Aliniagerdroudbari, Haniph, Alhadri, Muapper, Zakri, Waleed, Mohammed, Abdul Haq, Mahajan, Ajay, and Farhad, Siamak. "Fast Fault Diagnosis of a Lithium-Ion Battery for Hybrid Electric Aircraft." *Proceedings of the ASME 2018 Power and Energy Conference.* Lake Buena Vista, FL, USA, June 24-28, 2018.

[8] Nazari, Ashkan, and Nazari, Arash. "Experimental Investigation on Newtonian Drop Formation in Different Continuous Phase Fluids." *Proceedings of the ASME 2018 International Mechanical Engineering Congress and Exposition IMECE2018.* 2018.

[9] Mohammed, A., Alhadri, M., Zakri, W., Aliniagerdroudbari, H. et al. "Design and Comparison of Cooling Plates for a Commercial Pouch Lithium-ion Battery for Electrified Vehicles." *SAE International* 2018-01-1188, 2018.

[10] Zakri, Waleed, Alhadri, Muapper, Mohammed, Abdul Haq, Esmaeeli, Roja, Hashemi, Seyed Reza, Aliniagerdroudbari, Haniph, and Farhad, Siamak "Quasi-Solid Graphite Anode for Flexible Lithium-ion Battery." *Proceedings of the ASME 2018 Power and Energy* Lake Buena Vista, FL, USA.

[11] Oghbaei, Morteza, Baniasadi, Fazel, and Asgari, Sirous. "Lithium iron silicate sol–gel synthesis and electrochemical investigation." *Journal of Alloys and Compounds* Vol. 672 (2016): pp. 93-97.

[12] Choi, Yichul, Zheng, Husong, Baniasadi, Fazel, Tao, Chenggang, and Park, Kyungwha. "Effects of Intrinsic Surface Defects on Morphology and Electronic Structure of a Thin PtSe 2 Film from First-principles." *Bulletin of the American Physical Society* (2018).

[13] Alhadri, Muapper, Esmaeeli, Roja, Mohammed, Abdul Haq, Zakri, Waleed , Hashemi, Seyed Reza, Aliniagerdroudbari, Haniph, Barua, Himel, and Farhad, Siamak. "Studying Degradation of Lithium-Ion Batteries Using an Empirical Model for Aircraft Applications." *Proceedings of the ASME 2018 Power and Energy Conference.* Lake Buena Vista, FL, USA., 2018.

[14] Li, Kaiyuan, and Tseng, King Jet. "Energy efficiency of lithium-ion battery used as energy storage devices in micro-

grid." *Industrial Electronics Society, IECON 2015-41st Annual Conference of the IEEE.* 2015.

[15] Schimpe, Michael, Naumann, Maik, Truong, Nam, Hesse, Holger C, Santhanagopalan, Shriram, Saxon, Aron, and Jossen, Andreas. "Energy efficiency evaluation of a stationary lithium-ion battery container storage system via electro-thermal modeling and detailed component analysis." *Applied energy* Vol. 210 (2018): pp. 211-229.

[16] Meister, Paul, Jia, Haiping, Li, Jie, Kloepsch, Richard, Winter, Martin, and Placke, Tobias. "Best practice: performance and cost evaluation of lithium ion battery active materials with special emphasis on energy efficiency." *Chemistry of Materials* Vol. 28 No. 20 (2016): pp. 7203-7217.

[17] Toman, Marek, Cipin, Radoslav, Cervinka, Dalibor, Vorel, Pavel, and Prochazka, Petr. "Li-Ion Battery Charging Efficiency." *ECS Transactions* Vol. 74 No. 1 (2016): pp. 37-43.

[18] Lan, Chuanjin, Xu, Jian, Qiao, Yu, and Ma, Yanbao. "Thermal management for high power lithium-ion battery by minichannel aluminum tubes." *Applied Thermal Engineering* Vol. 101 (2016): pp. 284-292.

[19] Smith, Joshua, Hinterberger, Michael, Schneider, Christoph, and Koehler, Juergen. "Energy savings and increased electric vehicle range through improved battery thermal management." *Applied Thermal Engineering* Vol. 101 No. (2016): pp. 647-656.

[20] Zhao, Jiateng, Rao, Zhonghao, Huo, Yutao, Liu, Xinjian, and Li, Yimin. "Thermal management of cylindrical power battery module for extending the life of new energy electric vehicles." *Applied Thermal Engineering* Vol. 85 (2015): pp. 33-43.

[21] Lu, Languang, Han, Xuebing, Li, Jianqiu, Hua, Jianfeng, and Ouyang, Minggao. "A review on the key issues for lithium-ion battery management in electric vehicles." *Journal of Power Sources* Vol. 226 (2013): pp. 272-288.

[22] Nazari, Ashkan, and Farhad, Siamak. "Heat generation in lithium-ion batteries with different nominal capacities and chemistries." *Applied Thermal Engineering* Vol. 125 (2017): pp. 1501-1517.

[23] Cai, Long, and White, Ralph E. "Mathematical modeling of a lithium ion battery with thermal effects in COMSOL Inc. Multiphysics (MP) software." *Journal of Power Sources* Vol. 196 No. 14 (2011): pp. 5985-5989.

[24] Nazari, Ashkan, "Heat Generation in Lithium-ion Batteries." Master thesis. University of Akron, 2016.

[25] Arora, Pankaj, Doyle, Marc, Gozdz, Antoni S, White, Ralph E, and Newman, John. "Comparison between computer simulations and experimental data for high-rate discharges of plastic lithium-ion batteries." *Journal of Power Sources* Vol. 88 No. 2 (2000): pp. 219-231.

[26] Kumaresan, Karthikeyan, Sikha, Godfrey, and White, Ralph E. "Thermal model for a Li-ion cell." *Journal of The Electrochemical Society* Vol. 155 No. 2 (2008): pp. A164-A171.

[27] Bernardi, D, Pawlikowski, E, and Newman, John. "A general energy balance for battery systems." *Journal of The Electrochemical Society* Vol. 132 No. 1 (1985): pp. 5-12.